Improved Simulation of Photoresists Using New Development Models

R.R. Dammel, J.P. Sagan, E. Kokinda, N. Eilbeck,
AZ Electronic Materials, Clariant Corporation
C.A. Mack, *Finle Technologies, Austin, TX*
G.G. Arthur, *Rutherford/Appleton Laboratories/UK,*
C. L. Henderson, S. A. Scheer, B. M. Rathsack, and C.G. Willson,
Dept. of Chem. Engineering, University of Texas at Austin

Abstract
A new development rate model is proposed which is based on an equation derived by Huang, Reiser and Kwei for the concentration dependence of the dissolution rate of acidic resins in aqueous alkaline developers. This equation predicts cessation of development at a critical concentration c. Experiments in which the developer strength was varied show that the critical concentration c* is a linear function of the normalized sensitizer concentration m of positive-tone resists. The model is shown to reproduce the R(m) curves of conventional photoresists well, but it does not fully the unusual drop in the development rate curves at comparatively low relative sensitizer concentrations of m = 0.4 to 0.7 shown by high-performance resist systems. This physical phenomenon can be related to a selective dissolution effect in which the lower molecular weight component of the two-component resins typically used in these resists is leached out of the surface areas. The onset of this phenomenon leads to a sudden lowering of the resist dissolution rate which is described by the introduction of a "notch function."*

1. Introduction: Why do we need improved development rate models?

The exposure step in photolithography, complete with changes in absorbance and standing waves, is well described by the A, B, and C parameters of the Dill equations.[1] More recently, the inclusion of refractive index changes [2] has led to an even more rigorous description.[3,4] The second part of the image formation, the development step in which the latent image is transformed into the three-dimensional relief structure, is much less understood from a theoretical point of view. The dissolution rate is generally expressed as a function of the sensitizer concentration m, which may be directly obtained as a function of depth into the resist by a solution of the Dill equations. The procedures for the extraction of such data sets have recently been reviewed.[5] It is possible, and has indeed been done on occasion, to generate a lookup table for the dissolution rate R as a function of m. However, due to the often considerable scatter involved in the dissolution rate data, such an approach requires piecewise smoothing of the R data as a function of m, which may be quite laborious. It is therefore generally preferred to fit the data set to a functional dependence of R on m, the so-called R(m) curve.

The earliest models proposed for the R(m) curve were designed to give a representation of the data without attaching an obvious physical significance to the fit parameters. An example of such an R(m) function is the Dill dissolution rate model:

$$R(m) = exp\left(E_1 + E_2 m + E_3 m^2\right) \tag{1}$$

The "Original Mack model"[6] can be derived from a consideration of the photolysis kinetics of multifunctional diazonaphthoquinone PACs [7]; provided that only the fully photolyzed PAC molecules lead to a dissolution promotion:

$$R(m) = R_{max}\frac{(a+1)(1-m)^{\tilde{n}}}{a+(1-m)^{\tilde{n}}} + R_{min};$$
$$a = \frac{\tilde{n}+1}{\tilde{n}-1}\left(1-m_{th}\right)^{\tilde{n}} \tag{2}$$

0277-786X/98/$10.00

where m_{th} is the value of m at the inflection point of the curve, and ñ is the developer selectivity. From the derivation, ñ is expected to be equal to the number of DNQ moieties in the PAC; in practice, it is often much higher.

The "Enhanced Mack model" [8] yields a superset of the Original Mack model curve family:

$$R(m) = R_{resin}\,\frac{1+k_{enh}(1-m)^{\tilde{n}}}{1-K_{inh}(m)^{l}}; \tag{3}$$

$$R_{min} = \frac{R_{resin}}{1+k_{inh}};\quad R_{max} = R_{resin}\left(1+k_{enh}\right) \tag{4}$$

where k_{enh} is the rate constant for the enhancement mechanism, k_{inh} is the rate constant for the inhibition mechanism, ñ is the enhancement reaction order, l is the inhibition reaction order, and R resin is the dissolution rate of the resin. Its derivation is based on similar kinetic arguments but takes into account that dissolution promotion and inhibition branches may have different dissolution kinetics. The larger number of parameters leads to additional flexibility in the curve fitting.

For many conventional photoresists, all of the above models provide an adequate description of the R(m) curve, with the Enhanced Mack model being perhaps a first among peers. Many of the modern high-performance i-line resists, however, show a "notch" in the development rate curve at high sensitizer concentrations (m values) which is not adequately described by the currently employed development rate equations. This high-m notch is highly relevant to the imaging behavior of the resists because the region of low solubility is what determines the endpoint of the development process. A recent publication [9] has shown that the "notch" has a strong influence on the quality with which experimental results are reproduced by the simulation. It was shown that the reproduction of depth of focus, sidewall angles, and the definition of the tops of resist features all were significantly improved in the simulations if a manually edited parameter file with the "notch" was used instead of a standard dissolution rate equation.[9] However, as shown in Fig. 1, the conventional models (1) – (3) cannot accurately describe the behavior of R(m) in the notch region.

However, correct reproduction of the shape of the R(m) curve in the region of the notch is critical for quantitative predictions of resist performance. Figure 2 compares the simulation results for the Original and Enhanced Mack Models with those for a model with a correct description of the notch region and the experimental resist structures. While the conventional models predict that the 0.34 μm line&space features should be heavily sloped, and that 0.30 μm features can no longer be resolved on an 0.54 NA i-line stepper even with a slight overdose, the simulation results obtained with the model developed in this paper predict well resolved features with high wall angles for both, a prediction which is fully borne out by experiment.

The systematic overestimation of the dissolution rate at high m values which is inherent in the conventional models also leads to a reduction in the predicted process window. Figure 3 shows simulated Bossung plots and line shapes for 0.34 μm features on a 0.54 NA i-line stepper for the Enhanced Mack model fit of Figure 1, compared to results obtained with the notch-fitting model developed in this paper. The simulation using the Enhanced Mack model predicts a large negative bias of the isofocal line and poorer film thickness retention in the negative defocus range, both of which are a direct result of the non-zero dissolution rate at high m predicted by this model. The notch-fitting model (cf. Fig. 17) predicts a near-neutral isofocal line bias and a much higher focus latitude. The experimental results are much better described by the latter prediction (cf. Fig. 4), although the experimental isofocal line shows a slight negative bias instead of the predicted slightly positive one. The isofocal bias can be adjusted by further fine tuning of the shape of the R(m) curve in the notch region.

For a quantitative description of high performance resist behavior, it is therefore necessary to have a development rate equation that can accurately describe also the high-m region and the phenomenon of cessation of development observed there. We will show that an equation that predicts cessation of development can be derived from the equations governing

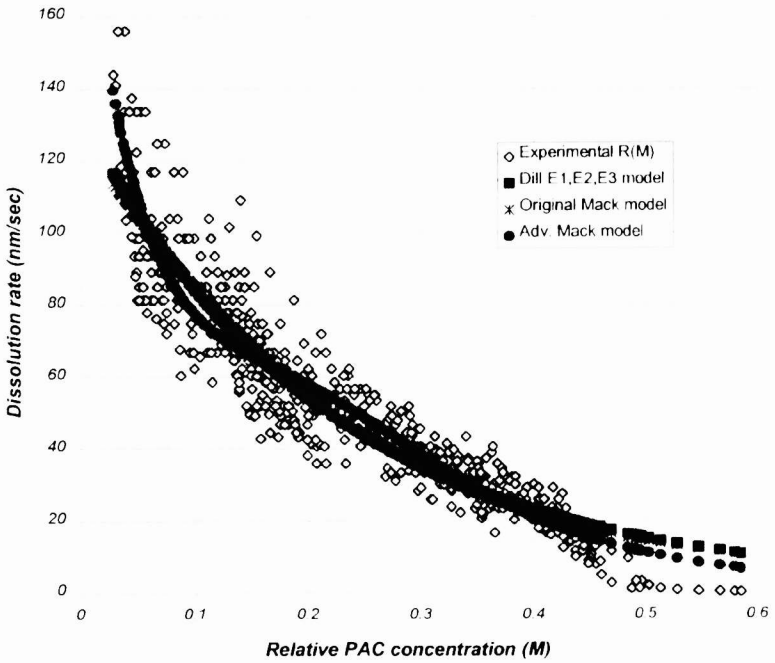

Figure 1: R(m) curve fit to development rate data for AZ® 7900 i-line resist (SB 90 °C, 90 sec, PEB 110 °C, 60 sec, development AZ® 300 MIF, 23 °C, 60 sec. Dill R(M) model: E_1= 4.8845, E_2= -4.5596, E3= 0.49154; Original Mack Model: R_{max}= 119.0, R_{min}= 4.15, m_{th}= -14.38, n= 7.9; Enhanced Mack Model: R_{resin}= 66.1, R_{max}= 140.0, R_{min}= 10^{-8}, n= 23.4, l= 3.76.

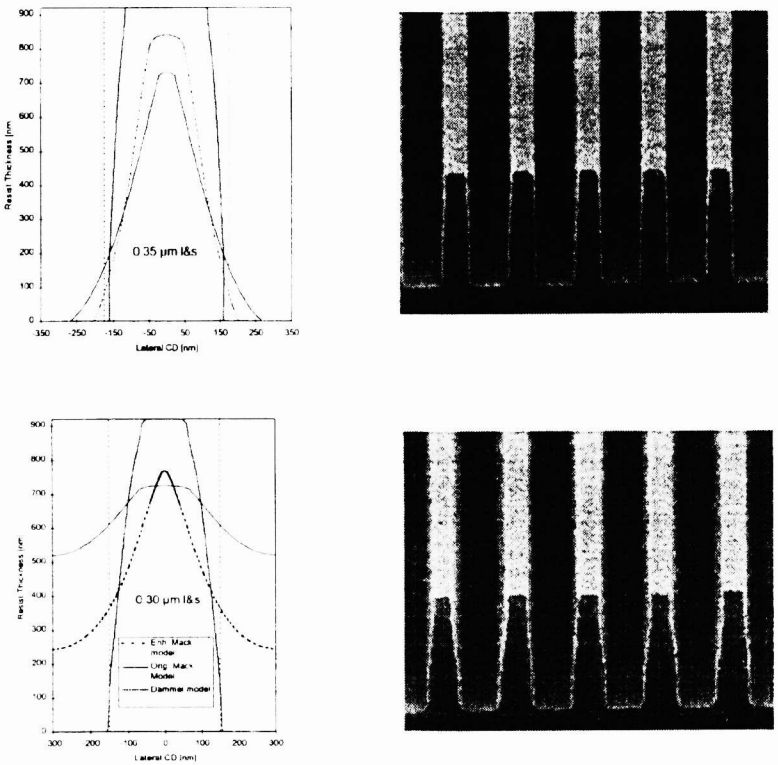

Figure 2: : a) (left) Prolith/2™ simulation of 0.35 µm and 0.30 µm features in AZ® 7900 resist for a slight overdose of 205 mJ/cm²; b) (right) experimental results (AZ® 7900 resist, 0.93 µm thick, 190 mJ/cm² i-line exposure, Nikon 0.54NA stepper, AZ300 MIF developer).

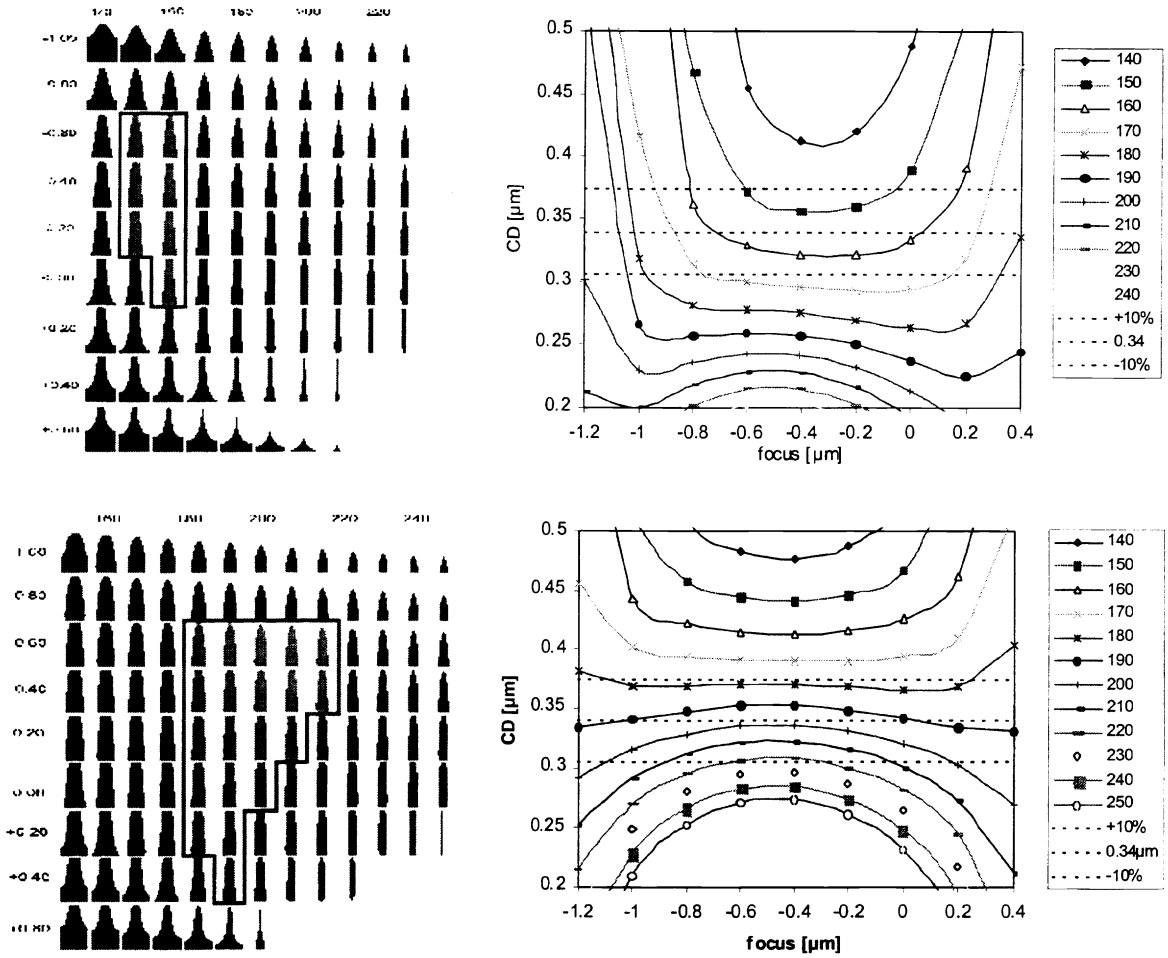

Figure 3: Comparison of process windows and Bossung plots obtained with the Enhanced Mack model of Fig. 1 (top) and the notch-fitting model of Fig. 17 (bottom).

the diffusion characteristics of the developer cations in the thin gel layer that forms at the resist/developer interface, the so-called penetration zone, but that the notch phenomenon involves further effects that require additional concepts to understand the physical phenomena occurring at the critical sensitizer concentration.

2. The New Development Model

2.1 The Critical Concentration Phenomenon

Huang, Reiser and Kwei [10] have studied the diffusion characteristics of the developer in the penetration zone. It was found that the diffusion of the counter cations is the rate limiting factor, apparently since the cations must completely shed their hydration sphere before they can enter into the resin. This leads to a dramatic decrease of the diffusion coefficient D close to the penetration zone/resin interface; using the depth x into the penetration zone, its decrease can be represented by $D = D_0(1-x)^{n/(n+1)}$. From this functional form, it is possible to derive an equation for the dependence of the dissolution rate on the developer concentration (Huang-Reiser-Kwei (HRK) equation) [10]:

$$R = \frac{D}{\delta} = \frac{\alpha \tilde{a}^n}{\delta} \frac{n+2}{(n+1)^2} \frac{(c-c^*)^{n+1}}{(c+c^*)} \tag{5}$$

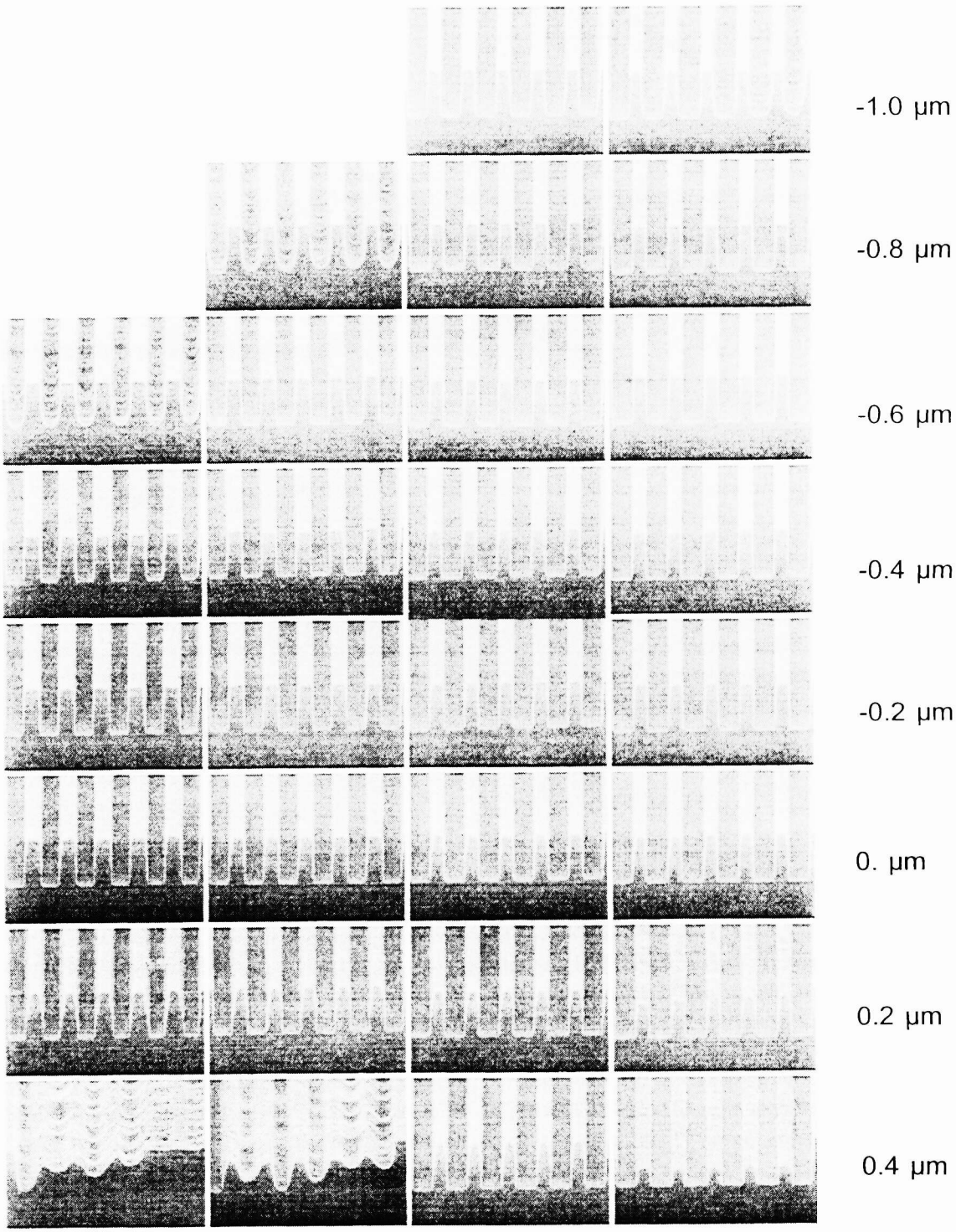

Figure 4: Focus-exposure matrix for 0.34 µm dense features printed in AZ®7900 resist (0.973 µm thick (E_{max}), 160-190 mJ/cm² i-line exposure, Nikon 0.54NA stepper, AZ300 MIF developer, 23 °C, 60 sec puddle).

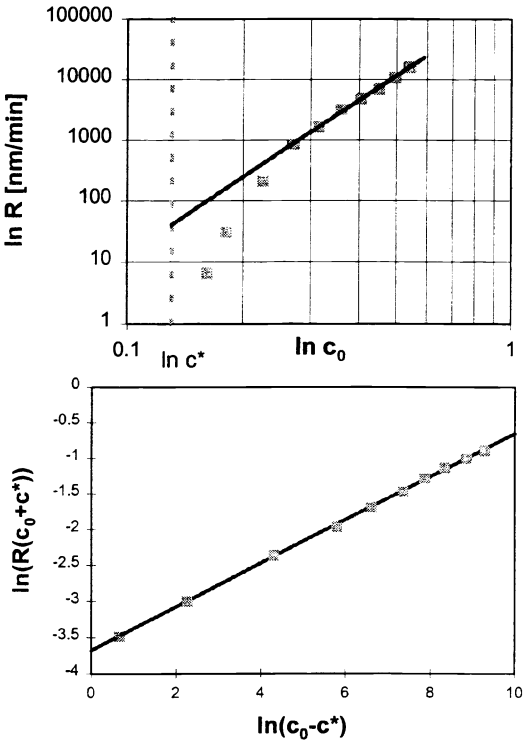

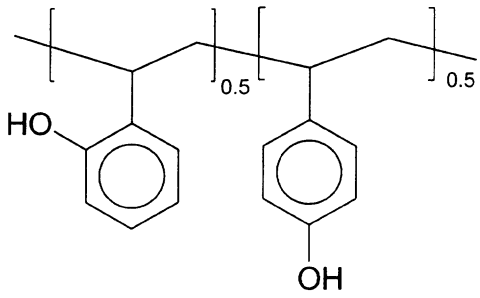

TMAH, 0.16 - 0.54 N

Figure 5: Comparison of the dissolution rates predicted by the standard power law with the HRK model close to the critical developer concentration for dissolution of a 1:1 2,4-hydroxystyrene copolymer in TMAH.

where δ is the thickness of the penetration zone, and c* is the critical concentration below which no development takes place. The value of c* can be determined by measuring dissolution rates in developers of varying strength and finding the concentration at which development ceases. The constant a corresponds to the proportionality factor of the base concentration of the developer at the penetration zone/developer interface to the bulk developer concentration: $c' = a\, c_0$. The physical meaning of n is given by the concentration dependence of the diffusion coefficient $D(c) = \alpha\,(c-c')^n$, with n/(n+1) also corresponding to the exponent of the position dependence of the diffusion coefficient in the penetration zone. The term $\alpha \cdot \tilde{a}^n/\delta$ is in the following abbreviated as a single term, k^n.

The HRK equation or variations thereof [11] can be shown to very accurately describe the dependence of the dissolution rate of phenolic resins on the developer normality, whether they are novolak [11], polyhydroxystryene [12], or unexposed and exposed photoresist. Figure 5 shows the improvement of the prediction of dissolution rates by the HRK equation over the power function law which has traditionally been applied. For low developer strength, the deviations from the power law become increasingly severe, until at the critical concentration c*, the dissolution rate tends asymptotically towards negative infinity. In contrast, the plot of $\ln(R\cdot(c_0-c^*))$ vs. $\ln(c_0-c^*)$ allows a correct description of low developer concentration since the singularity at c* has been shifted to negative infinity by the particular

We now apply the same approach to the photoresist. The unexposed (m=1) dissolution rate of many modern resists in standard 2.38% TMAH developer is zero, indicating that for these materials, c* is higher than the developer concentration (c=0.265 N). If the resist is irradiated with increased doses, dissolution will occur at some point, i.e., c* must be a function of the exposure state, or c* = c*(m). At the high-m end, the dissolution rate drops to zero at a sensitizer concentration m*, corresponding to the point between $0<m<1$ where c* first exceeds the developer concentration. For strongly exposed photoresist ($m<<m^*$), very fast dissolution occurs, and c* is certainly much smaller than 0.265 N.

From the above, it seems intuitively clear that the HRK model origin can in principle describe the phenomenon of cessation of development. Of course, not every resist will show this effect; there are a large number of resists that have non-zero dark film loss, which means that at m = 1, c* does not exceed the developer concentration used. The shape of the development rate equation will then follow from the HRK equation, provided that the actual dependence of c* on m is known.

An unspoken assumption of the model is that the composition of the resist is not changed by the developer as the resist develops. As we will see, this assumption is incorrect for an important class of resist materials, and additional efforts are necessary for the description of these resists. For now, however, we will continue the development of the model by investigating the dependence of c* on m.

2.2. Effects Of Exposure On c*

To obtain a functional dependence of c* on m, rate measurements need to be done in more and more dilute developers for exposed and post exposure baked resists at various exposure doses. The PEB is necessary to remove or at least strongly attenuate the standing wave so that only slowly varying m(z) values can be extracted from a simulation package such as PROLITH/2. Alternatively, the work can be carried out on a bottom antireflective coating to avoid standing waves altogether.

The dependence of c* on the developer strength can be obtained in an approximate way from contrast curve measurements in developers of different normalities c_0.[13] The energy E at which there is significant film loss is determined from an extrapolation of the film loss rate (Fig. 4); for this energy, c*(E) is then equal to the developer strength c_0. Measurements in a series of developers then yield the dependence of c* on E. Earlier investigations found a linear relationship between c* and the logarithm of the dose, ln E; from this relationship a fairly complicated formula could be derived:

$$c^*(m) = -b \cdot ln\, ln \frac{1}{(m+m_2)m_1} + a + b \ln C \qquad (6)$$

where C is the Dill bleaching rate parameter, and where m_1 and m_2 are additional constants required to prevent singularities at m = 0 and m = 1, with the additional constraints that $m_1 < 1/(1+m_2)$ and $m_1 m_2 < 1$.

Figure 7 illustrates the behavior of c*(m) according to Eq. (6). The bold curve shows the behavior for the a, b, and C values of obtained by a full curve fit to a data set derived from AZ®7900 contrast curves, with m_1 and m_2 values optimized by a fit to the full R(m) curve, while the thin curve corresponds to values of $m_1 = 1$ and $m_2 = 0$, i.e., the case for which there are singularities at m=0 and 1. As can be seen, the curves do not deviate substantially from each other except for very low or high m values (m > 0.9). In this case, the deviation for high m values is of no importance since the dissolution rate is zero for $c^* > c_0$ (0.265 N). In particular, the middle part of the curve (0.1 < m <0.8) is essentially linear. It is therefore possible to simplify the above model considerably by assuming a linear relationship between c* and m:

$$c^*(m) = \alpha + \beta m \qquad (7)$$

A determination of a set of R(m) curves for AZ7900 resist (Fig. 8) fully corroborates the simpler equation. The R(m) curves were determined in the way previously described [5]. For each developer strength, one obtains one R(m) curve the intercept of which yields the value of m* at which the development rate becomes zero; that particular developer normality is then the corresponding c*. A plot of the {c*,m} data pairs obtained from the different curves shows no discernible deviation from linearity (Fig. 9). By insertion of Eq. (7) into Eq. (5) it is now possible to directly fit the R(m) curves of positive resists with the new model. We will refer to this approach as to the linear Dammel model (LDM)

2.3. Tests Of The New Development Rate Equation

The LDM rate equation was first tested on the AZ®1500 and AZ®3300 photoresists. Both of these resist materials are not modern high-resolution resists but are targeted at larger geometries and higher photospeeds. For both of these resist materials, the new development model provides a good fit to the R(m) data, as do both the Original and Enhanced Mack models (Figs. 10 and 11). Both of them do not exhibit a "notch", and both of them do not reach zero development rate in the range of m values studied.

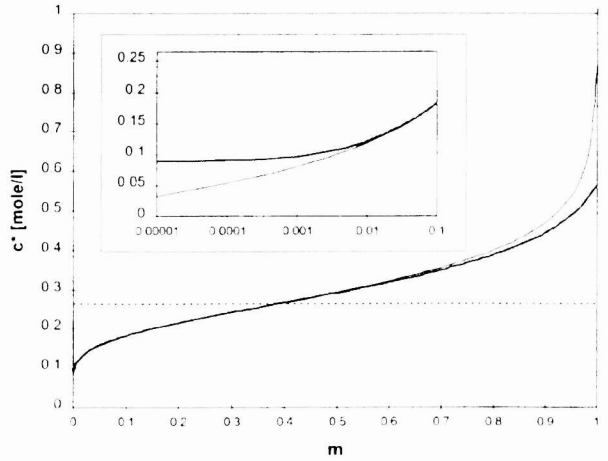

Figure 7: Comparison of c(m) curves according to Eq. (6)). Values used are: C = 0.0158, b = 0.0932, a = 0.6463. Bold curve: m_1 = 0.9994, m_2 = 0.0020, thin curve: m_1 = 1, m_2 = 0.*

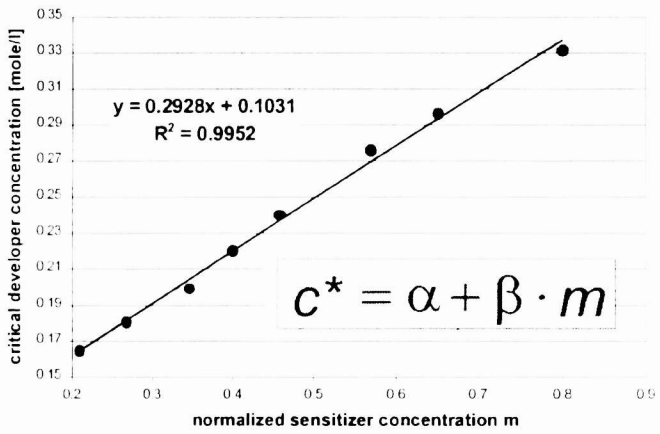

Figure 9: Linear relationship between c and m in the range 0.2 < m < 0.8. {c*,m} data pairs are obtained from data set in Figure 8.*

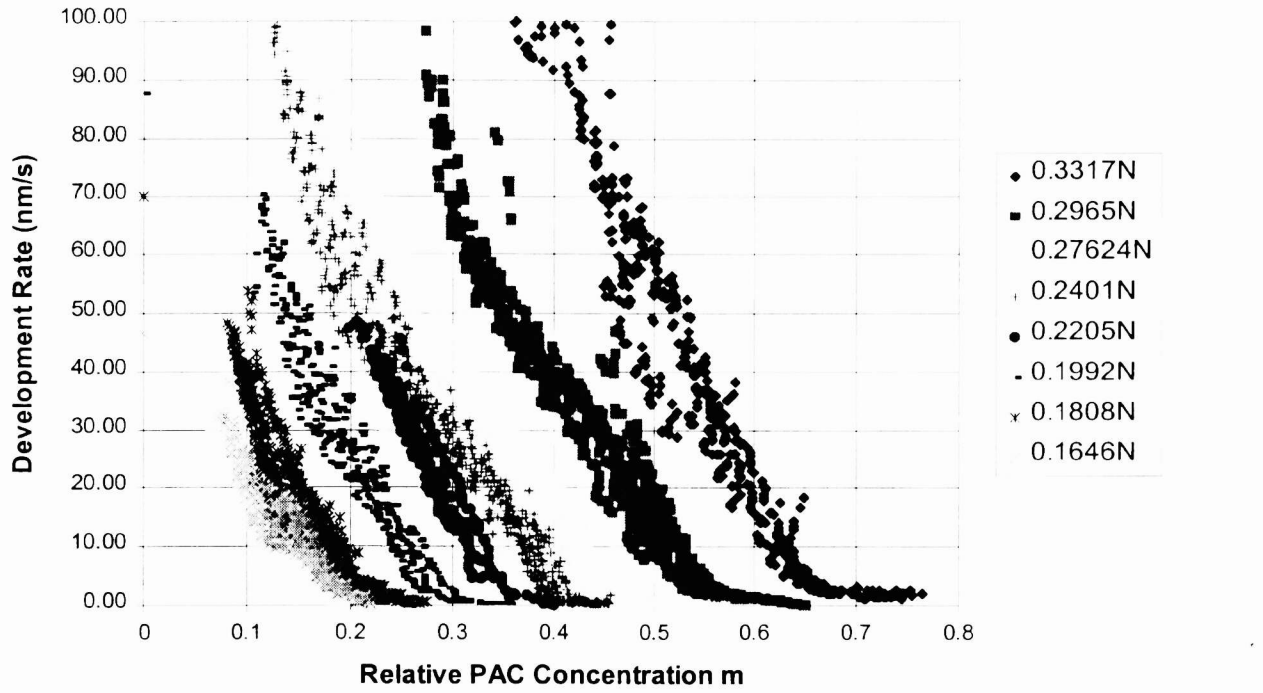

Figure 8: R(m) curve data of AZ® 7900 in developers of different normality.

If the development rate equation is applied to the AZ® 7900 high resolution i-line resist, one indeed obtains an R(m) curve that shows cessation of development at moderate m values (Fig. 12) when the experimentally determined constants of Fig. 9 are used. The general shape of the curve is correct but there is no "notch": although near-zero dissolution rates are reached at about the right point, the curve is too linear. It is possible to use a completely unconstrained fit to achieve a small improvement in non-linearity, but the constants are then found to be far removed from the experimental values and any physical significance. It therefore appears that an additional phenomenon must be operative in the low dissolution rate region that is causing the "notch". Evidence has indeed be presented for such a phenomenon in high-resolution resists, the so-called "selective dissolution effect".

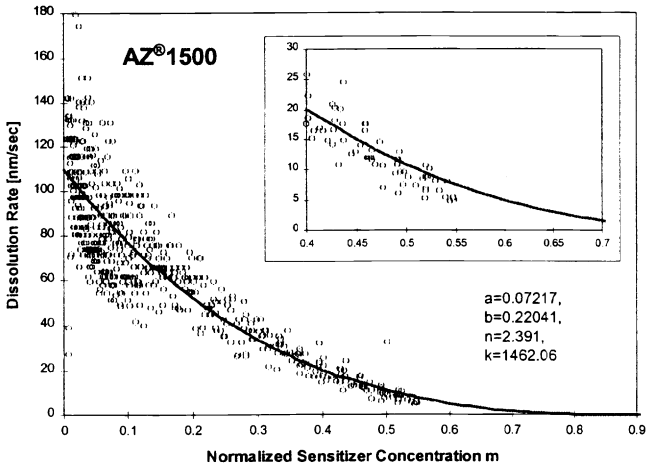

Figure 10: Linear Dammel model fit to the R(m) curve of AZ®1500resist

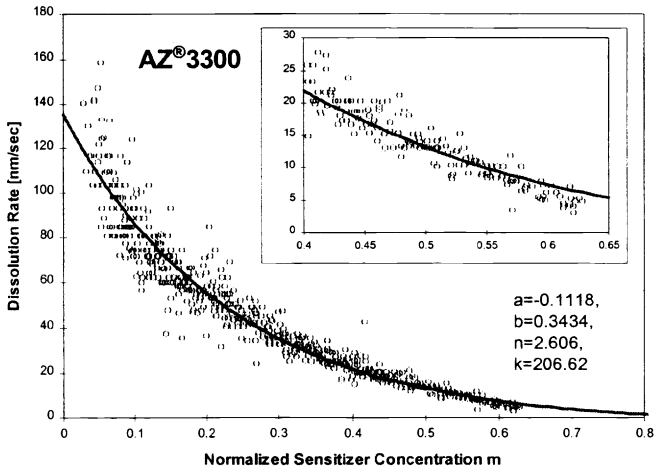

Figure 11: Linear Dammel model fit to the R(m) curve of AZ®3300 resist

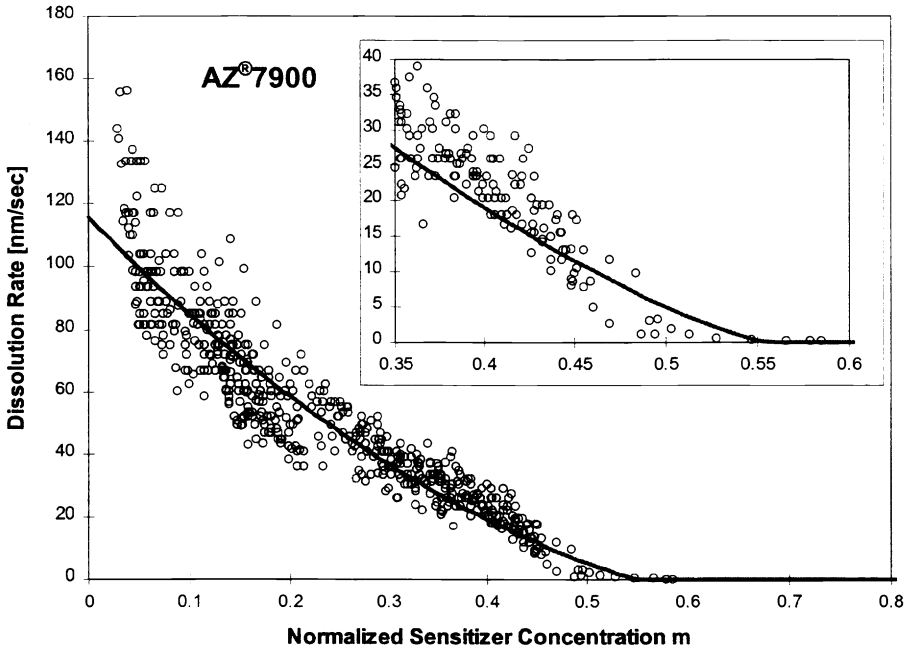

Figure 12: R(m) curve fit for AZ®7900 resist with the linear Dammel model. In this fit only the n and k parameters were allowed to vary; α and β parameters of the c(m) dependence were fixed at the exp. values of Fig. 9. Cf. Fig. 1 for a comparison with fits using the conventional models.*

3. Tandem Resins And The Selective Dissolution Effect

Classic DNQ/novolak resist design has been mired in a set of trade-off relationships, the most important of which are thermal stability vs. photospeed and inhibition strength vs. photospeed [15]. These trade-off relationships are already predicted by the secondary structure model [16], which relates the extent of intra-vs. intermolecular hydrogen bonding to the resin properties: novolak resins with a high proportion of ortho,ortho-methylene bridges have a high proportion of intramolecular hydrogen bonds; they are easily inhibited and yield high resolution, but show low thermal stability and photospeed. Changing the level of intramolecular hydrogen bonding to the opposite extreme yields high photospeed and thermal stability at the expense of the imaging quality. Classic resist design had to find a compromise between the two extremes, a task that not always led to a fully satisfactory conclusion.

Tandem Novolak Concept

trade-offs

	photo-speed	dark film loss	thermal stability
conventional novolak (H,M,L)	+	-	-
fractionated novolak (H,M)	0	0	0
fractionated novolak (H)	-	+	+
tandem novolak	+	+	+

Figure 13: Trade-off relationships in traditional resist design and the effect of the tandem novolak concept.

The way out of these trade-offs was shown to lie in the manipulation of the molecular weight distribution curve, i.e., in the use of fractionated resins [15]. Successive removal of the low and middle molecular weight parts of a resin first leads to a resist which is mediocre all around, then to one which has prohibitively low photospeed. The stroke of genius lay in re-adding the low to the high molecular weight fraction [15], resulting in a resin system which optimally combines all three previously incompatible target properties (Fig. 13). Since then, all high-resolution resist development has been a variation on this theme.

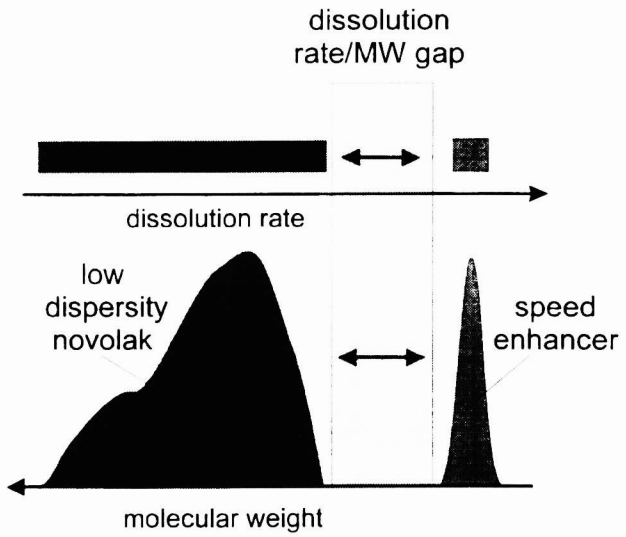

Figure 14: Molecular weight/dissolution rate distribution required for optimum resist performance in the tandem novolak scheme.

Beyond offering a way out of the trade-off relationships inherent in classic resist design, the tandem approach quite unexpectedly also yields a spectacular resolution enhancement. This was especially the case if it is not the low molecular weight fraction of the novolak which is added back to the high molecular weight fraction but a separately synthesized, well-characterized phenolic compound. With a non-novolak speed enhancer, it has proven easier to design its molecular structure for the best resist performance. Recent studies by researchers at Olin Microelectronics and Fuji Photo Film [17] have confirmed that as predicted by the tandem novolak concept, this effect is critically dependent on the molecular weight and the polydispersity of the novolak resin employed. Resolution enhancement was only observed if the molecular weight distribution of the resist was truly bimodal, i.e., if there was no overlap between the molecular weight distribution of the novolak and the speed enhancer. In Fig. 14, it is shown how such a bimodal molecular weight distribution can also lead to a bimodal dissolution rate distribution of the resin components.

Further investigations [17] tracing the concentration of a fluorine-substituted speed enhancer by XPS surface analysis showed that the speed enhancer concentration had decreased considerably in partially developed resist layers. This led to the formulation of the "selective dissolution model": in areas in which the total film dissolution rate is high, the speed enhancer dissolves homogeneously with the remaining components, and leads to an increase in the dissolution rate. For low dissolution rates, the speed enhancer is leached out of the film surface, leaving behind the low molecular weight compounds and leading to a large decrease in the dissolution rate (Fig. 15).

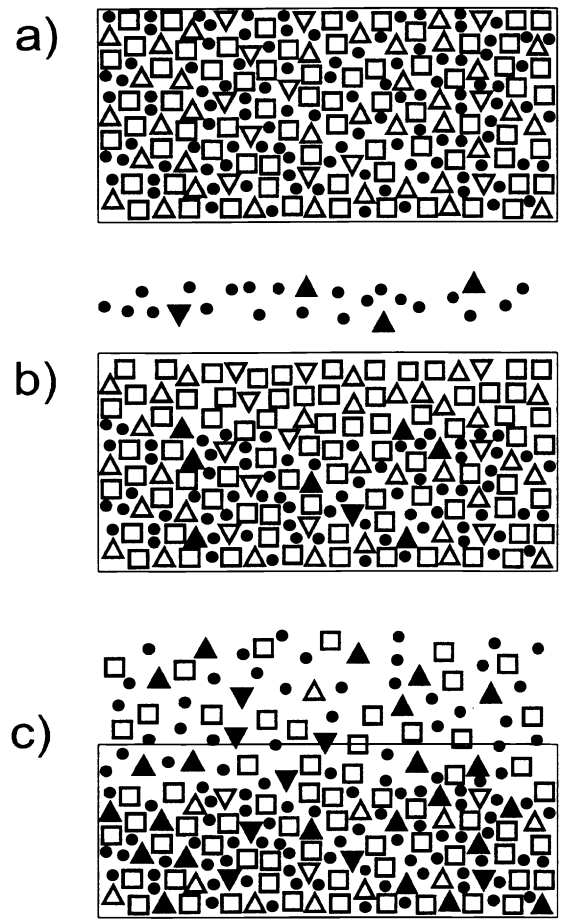

Figure 15: Selective dissolution effect in tandem novolak/speed enhancer resists. Squares: high MW resin, circles: low MW resin, open triangles: unexposed sensitizer, black triangles: exposed sensitizer. a) unexposed/undeveloped resist, b) partially exposed resist with formation of a speed enhancer depleted zone during development, c) strongly exposed resist showing homogeneous development at enhanced rate.

Researchers at JSR [18] have obtained results showing that for optimum resist performance, the dissolution rate should not vary much as a function of the depth into the resist, and that the dissolution rate as a function of dose should have a steep slope around the imaging dose. Both targets can be achieved with the use of phenolic additives in the tandem novolak concept.

4. Phenomenological Description of the Notch Effect By a Notch Function

The selective dissolution effect invalidates the basic premise underlying the assumption of the model in Eq. (5), i.e., that the composition of the resist is not changed by the developer. This assumption is exact when dealing with a monodisperse polymer, and may be presumed to be quite reasonable if one is dealing with any polymer lacking substantial very low molecular weight components. Indeed it is found that resists with polymeric speed enhancers generally do not exhibit notching. However, in the presence of monomeric speed enhancers, the leaching by the selective dissolution effect changes the resist composition in the vicinity of m = m*. The c*(m) values will then no longer follow the simple linear relationship of Eq. (7). Obviously it is not possible to describe this phenomenon with an unaltered model.

In the absence of a description of c* in the region of the notch, we have resorted to a phenomenological description of the notch effect. The dissolution rate curves are multiplied by a "notch function"

$$R_{notch}(m) = R(m) \cdot f_{notch}(m_{th\_notch}, n_{notch}) \tag{8}$$

an approach originally introduced by C. Mack [19], where f_{notch} is defined by

$$f_{notch} = \frac{(a'+1)(1-m)^{n_{notch}}}{a'+(1-m)^{n_{notch}}}; \qquad a' = \frac{n_{notch}+1}{n_{notch}-1} m_{th\_notch} \tag{9}$$

For values of m much smaller than m_{th_notch}, the notch function has values very close to 1, while for values of m much greater than m_{th_notch}, it approaches zero. The slope of the curve in the transition region centered on the m_{th_notch} inflection point is determined by n_{notch}. Figure 16 shows the shape of the f_{notch} functions for a variety of n_{notch} values.

The notch function can be used in conjunction with any development model, at the cost of adding two additional adjustable parameters. For the more advanced development models such as the Enhanced Mack model or the linear Dammel model, this brings the total number of adjustable parameters to 6. Attempts have therefore been made to use a simpler fit function [19], e.g.

$$R(m) = R_{max}(1-m)^n + R_{min} \tag{10}$$

The relative merits of different notch models have recently been compared [20]. However, there is no practical issue (such as, e.g., convergence problems) with using the larger number of parameters, since it is possible to obtain starting parameter

values by fitting the data for m values below the notch region with the 4-parameter model, and using the results as starting parameters for a full six-parameter fit including the notch region. In this paper, we will apply the notch function approach of Eq. (9) only to the Enhanced Mack model and the linear Dammel model.

Figure 17 shows the results of applying the notch function according to Eqs. (8-9) to the linear Dammel model. The fit function shown was obtained by an unconstrained fit of all six parameters. As can be seen, all regions of the experimental R(m) curve, including the notch area, are well described by the fit function. A similarly good fit is also obtained if the Enhanced Mack model multiplied by the notch function (Eq. (9)) is used as the fitting equation. The quality of the fit can be measured against that of the conventional models by comparison to Fig. 1.

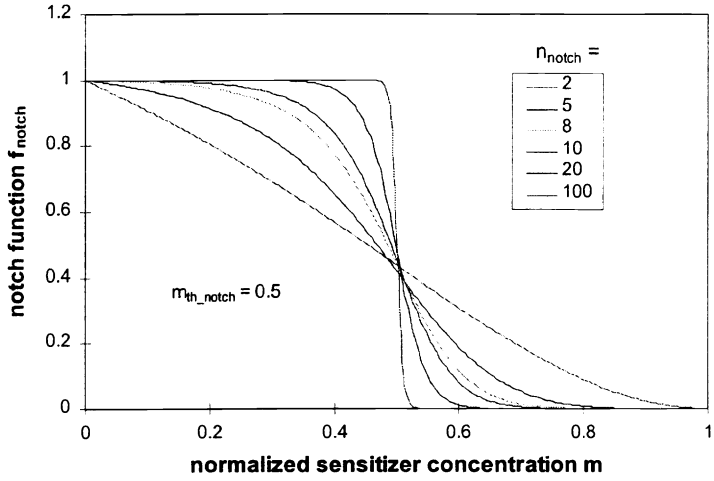

Figure 16:
Notch functions f_{notch} (cf. Eq. 9) for an m_{th_notch} value of 0.5 and n_{notch} values from 2 to 100.

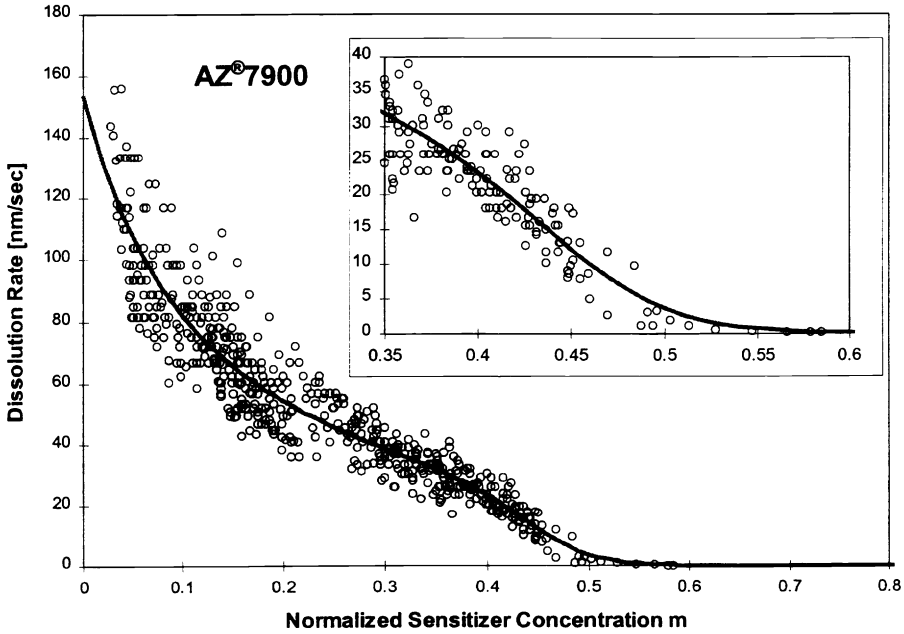

Figure 17:
R(m) curve fit for AZ®7900 resist according to the linear Dammel notch model.

Fit parameter:
α =-0.2629,
β= 0.01613,
n=15.73,
k=6885.5,
$m_{th\ notch}$=0.4467,
n_{notch}=15.86.

5. Prediction of R(m) Curves For Different Developer Strengths

Since the linear Dammel model explicitly contains the developer strength c_0, it is possible to describe an entire family of R(m) curves in developers of different normalities provided that the dependence of the fit parameters on c_0 is known. The data of Fig. 8 constitute such a family of R(m) curves that allow the necessary functional relationships to be determined.

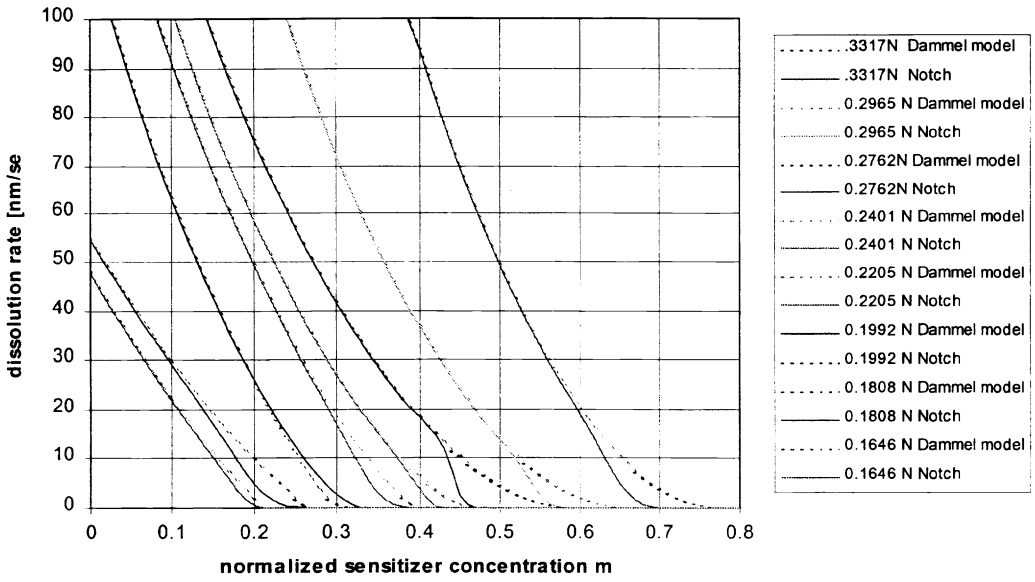

Figure 18: Fit of the data of Fig. 8 to the linear Dammel model and to the linear Dammel notch model for TMAH developer of normalities 0.1646 to 0.3317 N.

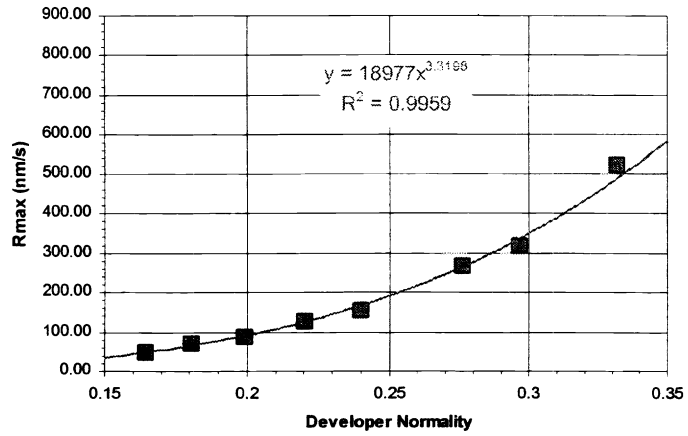

Figure 19: Dependence of maximum development rates $R_{max} = R(m=0)$ on TMAH developer normality

Fig. 18 shows the result of the fits of the data of Fig. 8 to the linear Dammel and linear Dammel notch models. Maximum notch strength is reached for 0.2762 N developer, i.e., at a slightly higher concentration than is used in standard 2.38% TMAH. Fig. 19 shows the dependence of the maximum dissolution rate $R_{max} = R(m=0)$ on c_0, and Fig. 20 show the dependence of the four adjustable parameters of the linear Dammel notch model which depend on c_0 (α and β are, of course, by definition independent of c_0). For R_{max}, the resist is fully exposed so that c0 is very large compared to c*. Under these conditions, Eq. (5) reverts to a simple power law (cf. Fig. 5), which is indeed the relation that is experimentally observed (Fig. 19). For three of the four adjustable parameters in Fig. 20 (n, m_{th_notch}, and n_{notch}), one finds that within the limits of the data set, linear relationships are a reasonably good description of the data, while the k parameter follows a power law in c_0. This means that for a complete description of the dissolution rate as a function of the resist exposure state and the developer normality, a total of six parameters are necessary for the linear Dammel model according to

$$R(m,c_0) = Fc_0^G \cdot \frac{D+Ec_0-2}{(D+Ec_0+1)^2} \cdot \frac{(c_0-a-bm)^{1+D+Ec_0}}{c_0+a+bm} \tag{11}$$

with four additional adjustable parameters describing the dependence of the notch effect on developer strength:

$$f_{notch} = \frac{(a'+1)(1-m)^{H+Kc_0}}{a'+(1-m)^{H+Kc_0}};\ a' = \frac{H+Kc_0+1}{H+kc_0-1}(L+Pc_0) \tag{12}$$

For a complete description of $R(m,c_0)$ in notching resists, one thus requires the rather large number of 10 adjustable parameters.

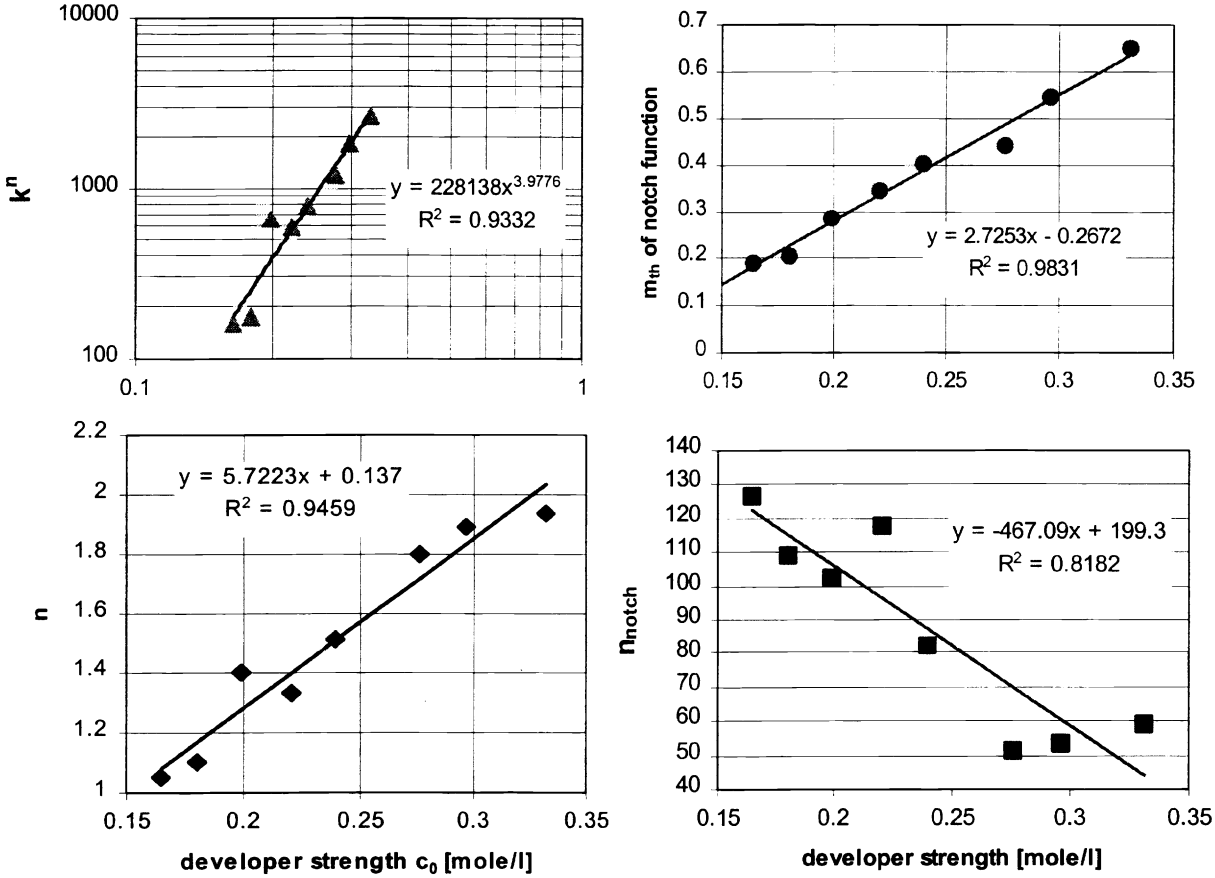

Figure 20: Behavior of the four adjustable parameters of the linear Dammel notch model which depend on c_0 as a function of developer normality.

6. Influence Of The Notch Parameters On Lithographic Bias

The influence of conventional resist parameters on Bossung plot reproduction has been investigated in the literature.[21] The overestimation of development rates for high m values that occurs in the conventional models leads to a large negative bias of the isofocal line (cf. Fig. 3, top). For strong notching behavior, one may find a positive bias (Fig. 3, bottom), so that somewhere in between there must be a point where the isofocal line has neutral bias. Since notching is described by the m_{th_notch} and n_{notch} parameters, the isofocal bias must also be a function of these parameters. In order to investigate this phenomenon, the Enhanced Mack model for AZ®7900 (cf. Fig. 1) was multiplied with notch functions f_{notch} for 2 values of m_{th_notch} (0.42 and 0.48) and 5 values of n_{notch} (5, 10, 20, 40, and 80). The shape of the corresponding notch functions is illustrated in Fig. 21 for the case of m_{th_notch} = 0.48. Prolith/2 simulations of Bossung plots were then carried out for the 10 resulting R(m) curves, and the isofocal line bias was determined. A plot of the results (Fig. 22) shows that for both values of m_{th_notch} used, the isofocal line has neutral bias at n_{notch} = 20. For lower values, the isofocal line has a quickly increasing negative bias, whereas for higher ones the bias is positive but increases with a lower slope. The higher m_{th_notch} value leads to a steeper response.

This case study indicates that it will be possible to adjust the isofocal line bias predicted by a resist simulation to the correct experimental value by tuning the value of n_{notch}. Such a tuning ability will result in a large improvement in the quality of quantitative predictions of resist behavior, since a large part of the deviations seen today are directly related to the reduction of the process window by an incorrect isofocal line bias. However, it is also evident from Fig. 21 that for low values of n_{notch}, the notch function as used today may have too long a range since it impacts development rates for values of m that are far from the notch region. This impact of the notch function can be compensated for by the other R(m) parameters but will lead to a loss of physical significance of the parameters.

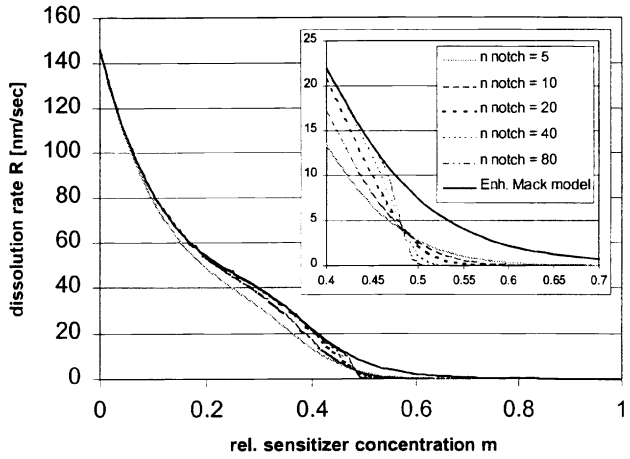

Figure 21: Shape of the R(m)·f_{notch}(m) functions for an m_{th_notch} value of 0.48 and n_{notch} values of 5 to 80.

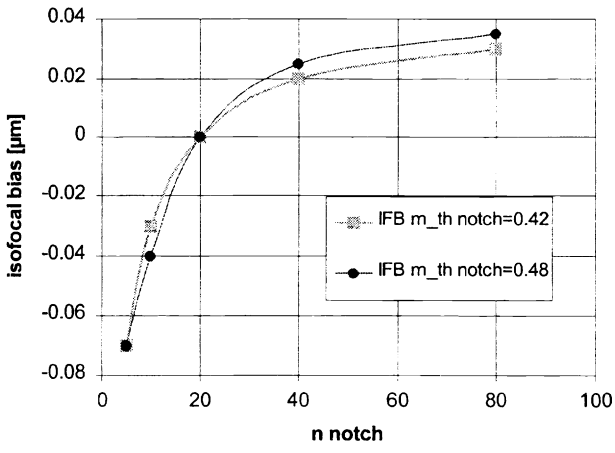

Figure 22: isofocal line bias (IFB) as a function of m_{th_notch} and n_{notch} (see text for details).

7. Discussion

The linear Dammel model given by Eq. (5) and (7) correctly describes the behavior of non-notching resists by parameter sets close to the experimental ones. It is the first physico-chemical description of the resist dissolution phenomenon in which all parameters have a clearly defined physical significance. Moreover, the same formalism allows to describe the developer strength dependence of the R(m) curve parameters, yielding a complete R(m, c_0) curve equation. For notching resists, an additional description of the leaching phenomenon is required in order to correctly reproduce the behavior both in the notching region, where leaching occurs, and in the non-notching regions, where leaching is minimal. The additional parameters are necessary to describe the effects of the selective dissolution mechanism which changes the composition of the resist through the leaching of the speed enhancer. The approach taken in this and other papers [20] is to introduce a notch function which describes the phenomenon in an empirical way. Such functions can be utilized to set up look-up tables or rate files for use in commercial simulators, and they are being incorporated in newer versions of simulation programs such as Prolith/2 Version 6. A minor blemish still exists in the fact that for n_{notch} values below 20, corresponding to the typical slightly negative isofocal bias values observed experimentally, the influence of the present notch function extends far beyond the notching region. Overcompensation by the R(m) curve parameter fit then leads to some loss of physical significance for these parameters. In the future, it may be possible to expand the linear Dammel model with a description of the behavior of c* in the notching region that overcomes this difficulty.

The concepts derived for the mechanism of action of high-performance resists in this publication and by previous authors [17] have both obvious and less obvious impacts on photoresist design. Especially for the notching" type of high-resolution resist, but also to a lesser extent for "non-notching" resists which reach zero development rate before high m values, it is clear that the resist profiles are essentially contour lines for a value of m = m*. However, if the profiles are iso-m* contours, then it follows that standing waves will seriously impact image formation and resist performance. It is indeed found that speed enhancer-containing resists do not show the benefits of the selective dissolution effect unless the resist process includes a PEB, or the exposure is done on a non-reflective substrate [17]. Moreover, it was found that those speed enhancers which are smaller and show a stronger depression of the glass transition temperature of the resist matrix also gave the best functional results [17]. It thus seems that with the new type of speed enhancers we have given the spiral of progress one full turn, and are back in a trade-off relationship similar to the one that resist design escaped from with the tandem novolak approach.

Understanding the effects of the shape of the R(m) curves on resist performance and relating them to the chemical structure and physical properties of the resist components by structure activity relationships constitutes the core of "R(m) curve engineering", a new way of looking at resist design that may help to push the final resolution limit of DNQ/novolak resists beyond the quarter-micron mark with existing steppers and without optical wavefront enhancements.

8. References

1) F.H. Dill, W.P. Hornberger, P.S. Hauge, and J.M. Shaw, IEEE Trans. Electron Devices **22**(4), 445-452 (1975).
2) C.L. Henderson, C.G. Willson, R.R. Dammel, and R.A. Synowicki, Proc. SPIE **3049** 585-595 (1997).
3) A. Erdmann, C.L. Henderson, C.G. Willson, and W. Henke, Proc. SPIE **3049**, 529-540 (1997).
4) A. Erdmann, C.L. Henderson, C.G. Willson, and W. Henke, Proc. SPIE **3048**, 114-124 (1997).
5) C.L. Henderson, S.N. Pancholi, S.A. Chowhury, K.D Dombrowski, C. G. Willson, and R.R. Dammel, Proc. SPIE **3049**, 805-815 (1997); C.L. Henderson, S.N. Pancholi, S.A. Chowhury, C. G. Willson, and R.R. Dammel, Proc. SPIE **3049**, 816-828 (1997); C.L. Henderson, P.C Tsiartas, S.N. Pancholi, S.A. Chowhury, K.D. Dombrowski, A.M. Chinwalla, C.G. Willson,, Proc. SPIE **3049**, 212-223 (1997).
6) C. Mack, J. Electrochem.Soc. **134**(1), 148-152 (1987)
7) P. Trefonas and B.K. Daniels, Proc. SPIE **771**, 194-210 (1987); P. Trefonas and C. Mack, Proc. SPIE **1466**, 117-131 (1991)
8) C. Mack, J. Electrochem. Soc. **139**(4), L35-L37 (1992); C.A. Mack, "*Inside Prolith*™", Finle Technology, Austin, TX 1997, ISBN 0-9650922-0-8, p. 106ff.
9) G. Arthur, B. Martin, and C.A. Mack, Proc. SPIE **3049**, 189-200 (1997).
10) J.-P. Huang, T.K. Kwei and A. Reiser, Proc. SPIE **1086**, 74 (1989); Macromolecules **22**, 4106 (1989).
11) T.F. Yeh, H.Y. Shi, A. Reiser, M.A. Toukhy, and B.T. Beauchemin, Jr., J. Vac. Sci. Technol. B **10**, 715 (1992).
12) R. Dammel, M.D. Rahman, P.H. Lu, and V. Elango, Polym. Adv. Technol. **5** (1), 28-40 (1994); R.R. Dammel, M.D. Rahman, P.H. Lu, A. Canize, and V. Elango, Proc. SPIE **2195**, 542-557 (1994).
13) R.R. Dammel, J. Photopolym. Sci. Technol. **10**, 1997; R.R. Dammel, J. Sagan, E. Kokinda, and N. Eilbeck, Proc. Photopolym. Conf. (1997), in print.
14) A. Reiser, H.-Y. Shi, T.-F. Yeh, and J.-P. Huang, Angew. Chem. Intl. Ed. **35**(21), 2413-2548 (1996).
15) M. Hanabata, F. Oi, and A. Furuta, Proc. SPIE **1466**, 132-140 (1991); M. Hanabata, F. Oi, and A. Furuta, Proc. SPE Reg. Tech. Conf. Photopolym. (Ellenville) **1991**, 77-90.
16) M.K. Templeton, C.R. Szmanda, and A. Zampini, Proc.SPIE **771**, 136 (1987).
17) Y. Kawabe, S. Tan, F. Nishiyama, S. Sakaguchi, and Tadayoshi Kokubo, A. Blakeny and L. Ferreira, Proc.SPIE **2724**, 420-437 (1996).
18) H. Miyamoto, T. Nakamura, K. Inomata, T. Ota, and A Tsuji, Proc. SPIE 2438, 223-234 (1995). K. Douki, T. Kajita, and S. Iwanaga, Proc. SPIE **3333**, (1998), in print.
19) G. Arthur, C.A. Mack, and B. Martin, Olin Microlithography Seminar, Interface'97, Nov. 1997, 55-66.
20) G. Arthur, C. Wallace, and B. Martin, Proc. SPIE **3333**, in print.
21) G. Arthur and B. Martin, Proc. SPIE **2725**, 85-93 (1996).